Materials Science and Engineering C 57 (2015) 314–320

Contents lists available at ScienceDirect

Materials Science and Engineering C

journal homepage: www.elsevier.com/locate/msec

Poly(lactic acid)/TiO_2 nanocomposites as alternative biocidal and antifungal materials

Carmen Fonseca [a], Almudena Ochoa [a], Maria Teresa Ulloa [b], Eduardo Alvarez [b], Daniel Canales [c], Paula A. Zapata [c,*]

[a] POLCA, Departamento de Ingeniería Mecánica, Química y Diseño Industrial, Escuela Técnica Superior de Ingeniería y Diseño Industrial, Universidad Politécnica de Madrid, Ronda de Valencia 3, Madrid, Spain
[b] Programa de Microbiología y Micología. ICBM-Facultad de Medicina Universidad de Chile, Dirección, Avenida Independencia 1027, Comuna Independencia, Santiago, Chile
[c] Grupo Polímeros, Facultad de Química y Biología, Universidad de Santiago de Chile, USACH, Casilla 40, Correo 33, Santiago, Chile

ARTICLE INFO

Article history:
Received 31 March 2015
Received in revised form 23 June 2015
Accepted 31 July 2015
Available online 7 August 2015

Keywords:
Nanocomposites
Polymer matrix composites (PMCs)
Nano particles
Mechanical properties
Thermal properties

ABSTRACT

Poly(lactic acid) (PLA) composites with titanium oxide (TiO_2) ~10-nm nanoparticles were produced by the melting process and their main properties were evaluated. The nanoparticles are homogeneously dispersed in the matrix with a low degree of agglomeration, as seen by transmission electron microscopy (TEM). The crystallinity temperature increased ~12% when 5 wt.% of TiO_2 was added, showing that the nanoparticles acted as nucleating agents this trend was confirmed by optical images. The elastic modulus increased ~54% compared to neat PLA at 5 wt.% of nanoparticles. Despite these improvements, PLA/TiO_2 nanocomposites showed lower shear viscosity than neat PLA, possibly reflecting degradation of the polymer due to the particles. Regarding biocidal properties, after 2 h of contact the PLA/TiO_2 composites with 8 wt.% TiO_2 showed a reduction of *Escherichia coli* colonies of ~82% under no UVA irradiation compared to pure PLA. This biocidal characteristic can be increased under UVA irradiation, with nanocomposites containing 8 wt.% TiO_2 killing 94% of the bacteria. The PLA/TiO_2 nanocomposites with 8 wt.% were also 99.99% effective against *Aspergillus fumigatus* under the UVA irradiation.

1. Introduction

One of the most promising biopolymers able to replace petroleum-derived polymers used in industrial applications is poly(lactic acid) (PLA), which is a linear aliphatic thermoplastic polyester derived from 100% renewable resources such as sugar, corn, potatoes, and beet. The most common route for industrial production of high molecular weight PLA is the ring-opening polymerization (ROP) of the lactide monomer formed from lactic acid, which is produced by fermentation of renewable agricultural resources [1]. PLA is easily processed into a desired configuration on standard plastics processing equipment to yield moulded parts, films or fibres. Owing to these properties, PLA has a wide range of potential industrial applications, and it is a candidate for use in packaging due to its transparency, processability, low toxicity, and environmentally benign characteristics. Although nowadays the cost of PLA production is relatively high compared to that of some conventional petroleum-derived plastic products, it can be predicted that this status will change as its demand and production volumes increase with time [2].

Compared to commodity polymers such as polyethylene, polypropylene and polystyrene, the mechanical properties of semi-crystalline PLA are attractive, particularly its Young's modulus, making it an excellent substitute for commodity polymers in short-term packaging [3]. The main disadvantage of PLA is its low crystallization ability, which limits significantly its industrial implementation in different applications [4]. One route to overcome this disadvantage is the incorporation of nanoparticles into the PLA matrix, yielding nanocomposites that can give new properties to the polymer [5]. For example, modification of a polymeric matrix such as PLA to prevent growth or reduce adhesion of detrimental microorganisms is a highly desired objective. Hence, there is significant interest in the development of antimicrobial biomaterials for application in the packaging of medical devices and food [6]. Different nanoparticles such as silver [7], copper [8], and recently TiO_2 nanoparticles [9–12] have been incorporated into polymers, in order to obtain biocidal properties. The incorporation of nanoparticles like TiO_2 into the PLA polymer is attractive because TiO_2 has odour inhibition and self-cleaning mechanisms. Furthermore, they are inert, non-toxic and inexpensive materials, with a high refractive index and a high ability to absorb UV light. TiO_2 excited by light with a radiation input greater than the particular band gap energy of the TiO_2 crystal (3.2 eV for anatase; 3.03 eV for rutile) generates pairs of holes (h^+) and electrons (e^-) by molecular excitation, which can migrate to the surface of the catalyst to react with water and oxygen, generating hydroxyl radicals ($OH^{\cdot}$) and reactive oxygen species able to degrade cell components of microorganism and act as anti-bacterial agents.

* Corresponding author.
E-mail address: paula.zapata@usach.cl (P.A. Zapata).

http://dx.doi.org/10.1016/j.msec.2015.07.069
0928-4931/

The influence of TiO_2 incorporation into PLA in order to study its antimicrobial and antifungal behaviour has been scarcely reported. Anatase titanium dioxide (TiO_2) nanoparticles (0.1 to 5 wt.%) were loaded into polylactide (PLA) by the melt intercalation method. Nanocomposite films had bacteriostatic activity against *Klebsiella pneumoniae* (ATCC 4352) and *Staphylococcus aureus* (ATCC 6538). Increasing the filler content caused a noticeable difference in the tensile stress and decomposition temperature of the films [13].

The reports are usually based on the study of the influence of the incorporation of TiO_2 on the thermal and mechanical properties. The surface treatment of TiO_2 nanoparticles (g-TiO_2) by the melt process was carried out in the presence of lactic acid in order to improve the dispersion of TiO_2 nanoparticles within the PLA [14,15]. The introduction of TiO_2 into the PLA matrix improved PLA crystallinity and played an important role in the improvement of the mechanical properties [16].

PLA nanocomposites with covalent bonding between the TiO_2 nanowire surface and PLA chains were synthesized by in situ melt polycondensation. The grafted PLA chains had significantly increased glass transition temperature and thermal stability compared to pure PLA. TEM micrographs showed homogeneous dispersion of TiO_2 nanowires in the PLA matrix [15].

Therefore, the effect of different amounts of TiO_2 on the thermal, mechanical, and shear viscosity properties of PLA was studied. The antimicrobial and antifungal behaviour of these PP/TiO_2-Ntbs nanocomposites against *Escherichia coli* and *Aspergillus fumigatus* were also investigated.

1.1. Experimental

1.1.1. Materials

Poly(lactic acid) constitute in the majority for an L-isomer with 95.7% was purchased from Nature Works LLC (Spain). PLA pellets with a density of 1.24 g/cm^3 and a melt mass flow rate (MFR) of 6 g/10 min. TiO_2 nanospheres were synthesized using the sol–gel method. The procedure for the synthesis of TiO_2 nanoparticles was reported in a previous paper [17].

1.2. PLA/TiO_2 nanocomposite preparation

The preparation of PLA and PLA/TiO_2 nanocomposites was carried out in a roller mixer (GUIX) at 170 °C during 10 min following the standard UNE-EN 1417:1997 + A1:2008. Before preparing the nanocomposites, the PLA was dried in a vacuum oven at −0.5 bar during 2 h at 90 °C. The nanocomposites contained 1, 3, 5 and 8 wt.% of the nanoparticles.

1.3. PLA/TiO_2 nanocomposite characterization

The XRD patterns of the TiO_2 nanoparticles were obtained on a Siemens D5000 diffractometer, using Ni-filtered Cu Kα radiation (λ = 0.154 nm).

UV absorption spectra of the TiO_2 nanoparticles powders were measured on a Perkim Elmer Lambda 650 UV/Vis spectrometer. The UV spectra measurements were conducted within the 200–700 nm range. The band gap (Eg) energies were calculated according to the equation Eg = 1239.6/λg [18].

The melting temperature and enthalpy of fusion of the neat PLA and PLA/TiO_2 nanocomposite samples were measured by differential scanning calorimetry (DSC) (Mettler-Toledo DSC 823E). The samples were heated from 20 °C to 185 °C at a rate of 5 °C/min. The readings were taken from the second heating curve. The percentage crystallinity was calculated using the enthalpy of fusion of an ideal PLA with 100% crystallinity [16].

Thermal stability was characterized using Netzsch-TG209 F1 Libra (Netzsch, Germany) thermogravimetry (TG) under nitrogen and air atmospheres. Samples of 5 mg were heated from 30 °C to 600 °C at a heating rate of 20 °C /min.

Polymer viscosity was measured by dissolving the polymer in chloroform at 25 °C in an Ubbelohde viscometer. The Mv values were obtained from the Mark–Kuhn–Houwink equations and the values of the constants were K: $5.45 \cdot 10^{-4}$ dL g^{-1} and 0.73.

The morphology of the TiO_2-Ntbs and their dispersion in the composites were analyzed by TEM (JEOL ARM 200 F) operating at 20 kV.

The materials were moulded for 14 min in a hydraulic press, GUIX Mod GX 1103, at a maximum pressure of 180 kg/cm^2 and a temperature of 190 °C, following the UNE-EN ISO 293 standard.

The tensile properties of the polymer and nanocomposites were determined at a nominal strain rate of 50 mm/min and 1 mm/min to determine the tensile modulus of elasticity using a Hounsfield Universal Testing Machine, mod. H10KT.

Capillary rheometry

Shear stress and shear viscosity of neat PLA and its nanocomposite PLA were determined with a sweep of shear rates ranging from 10 s^{-1} to 4500 s^{-1} at 190 °C, using a capillary rheometer (Rosand RhV7, Rosand Precision Ltd). The composite was compressed at a speed of 20 mm/min up to a pressure of 0.5 MPa.

The isothermal spherulite growth rate of neat PLA and its nanocomposite was studied under a Leica DML optical microscope with polarized light coupled with a Linkam Scientific Instruments TMS94 heating stage controlled by a Linkam LTS 350 system. Thin sample pieces placed under a cover glass on a microscope slide were heated to 190 °C and kept for 2 min. The samples were then cooled to a given crystallization temperature.

Antimicrobial and antifungal properties

The antimicrobial effect of the different samples was determined using the ISO 20143 plate count method as was reported previously [12]. *E. coli* ATCC 25922 was used for the analysis. From a fresh culture, a microbial suspension of 1×10^5 CFU/mL by bioMérieux® Densimat was prepared in BHI broth plus Triton 100× in a humid chamber. The percentage inhibition of microorganism in the samples was determined according to their respective controls. Antifungal Properties were determinated using the same methodology of antimicrobial properties. *A. fumigatus* ChFC 166–1 was used for the analysis. Inocula were prepared according to CLSI guidelines. Each sample was recovered by suspending in 10 mL of sterile saline and serially diluted 1/10, 1/100, and 1/1000, and 0.2 mL of each dilution was plated in duplicate on Sabouraud agar plates and incubated at 37 °C for 72 h [19]. The percent reduction of the colonies was calculated using the following equations, which relate the number of colonies from the neat polymer (PLA) with the number of colonies from the nanocomposites (PLA/TiO_2).

The percent reduction of the colonies was calculated by the following equations, which relate the number of colonies from the neat polymer (PLA) with the number of colonies from the nanocomposites (PLA/TiO_2).

$$\%R = \frac{(CFU\ neat\ Polymer - CFU\ nanocomposite)}{(CFU\ neat\ Polymer)} \times 100 \quad (1)$$

2. Results and discussion

2.1. Characterization of nanocomposites

Fig. 1 displays the TEM images of TiO_2 and PE/TiO_2 nanocomposites. TiO_2 nanoparticles were obtained by the sol–gel method with spherical morphology and a diameter of ~10 nm. The TiO_2 nanoparticles were uniformly dispersed in the PLA matrix without obvious agglomeration, although under increased TiO_2 incorporation (8 wt.%) certain regions shown some agglomerations up to 0.5 μm. These results show that the

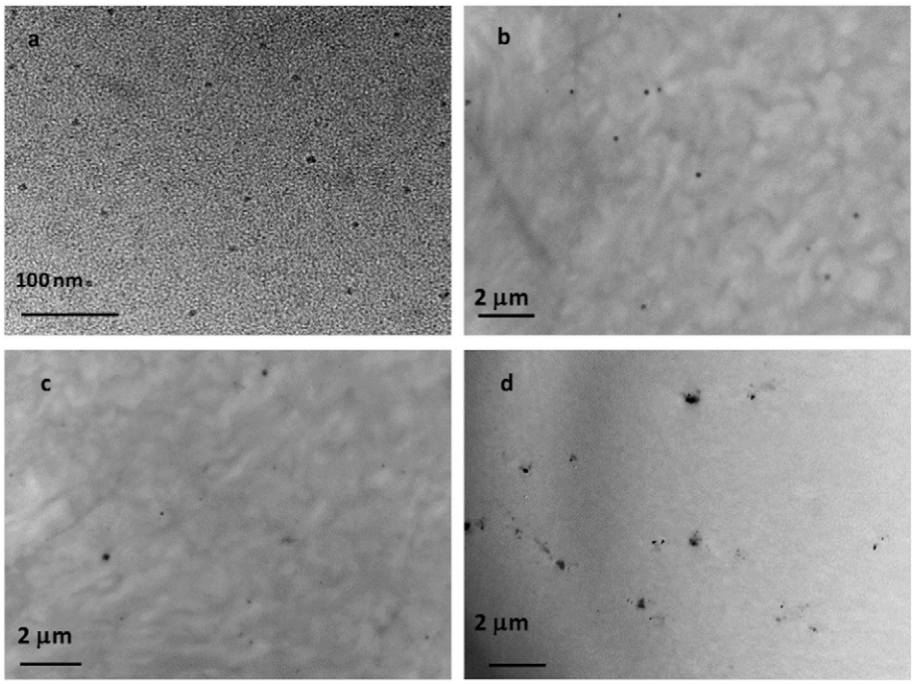

Fig. 1. TEM images of nanocomposites: (a) TiO_2 nanoparticles; (b) PLA/TiO_2 with 3 wt.%; (c) PLA/TiO_2 with 5 wt.%; and (d) PLA/TiO_2 with 8 wt.%.

homogeneous PLA/TiO_2 nanocomposites can be effectively produced by the melting process. On the other hand, by DRX and UV analysis it was evidenced that the nanoparticles corresponded to the anatase crystallinity phase [9].

The XRD pattern and UV absorption of the TiO_2 nanoparticles are displayed in Fig. 2. The diffractogram of the nanoparticles showed Bragg's reflection at 25, 38, 48, 54, 63, 70, and 75°, corresponding to the (101), (004), (200), (211), (204), and (220) tetragonal crystal planes of the anatase phase of TiO_2 [20]. A small diffraction peak at 31° is also displayed, corresponding to a small fraction of brookite. TiO_2 also presented a UV absorption around λg: 387 nm (Fig. 2), corresponding to an energy band gap (Eg) of 3.2 eV. The Eg values of TiO_2 nanoparticles were close to the value reported for the anatase phase. This band gap is related to the transition of valence electrons characteristic of TiO_2 [21,22].

2.1.1. Thermal and stability analysis of nanocomposites

Fig. 3 and Table 1 shown the thermal properties of the PLA and PLA/TiO_2 nanocomposites. PLA glass transition (Tg), followed by polymer crystallization (Tc) and polymer melting temperatures can be seen in the thermograms of all samples. The glass transition temperature around 60 °C for PLA and PLA/TiO_2 nanocomposites was close to that reported in the literature [23,24]. There was no change of Tg with the incorporation of nanoparticles.

The crystallization temperatures (Tc) increased from 106 °C for pure PLA to 120 °C for PLA/TiO_2 nanocomposites, showing that the addition of TiO_2 nanoparticles promoted PLA crystallization. Similar to other results, TiO_2 particles can act as nucleating centers, improving the crystallization ability of PLA [25]. Zou et al. [26] found that with the incorporation of talc (4 wt.%) to PLA the polymer showed an improve in the crystallization temperature until 20.8%, and its effect was more notorious with the incorporation of agent nucleating to the PLA/talc composite. Pan et. al [27] reported that with decreasing molecular weight the crystallization peak, Tc, shifts to higher temperature, indicating that the crystallization rate increased with decreasing molecular weight, and it is correlated with the viscosimeter molecular weight shown in Table 2.

The percent crystallinity of PLA did not show a significant change with nanoparticle incorporation. The melting temperature of neat PLA and PLA/TiO_2 nanocomposites with 1 and slight with 5 wt.% of TiO_2 nanoparticles presented two distinct peaks at 150 and 157 °C, ascribed to polymorphism of different crystal forms [27]. The low-temperature

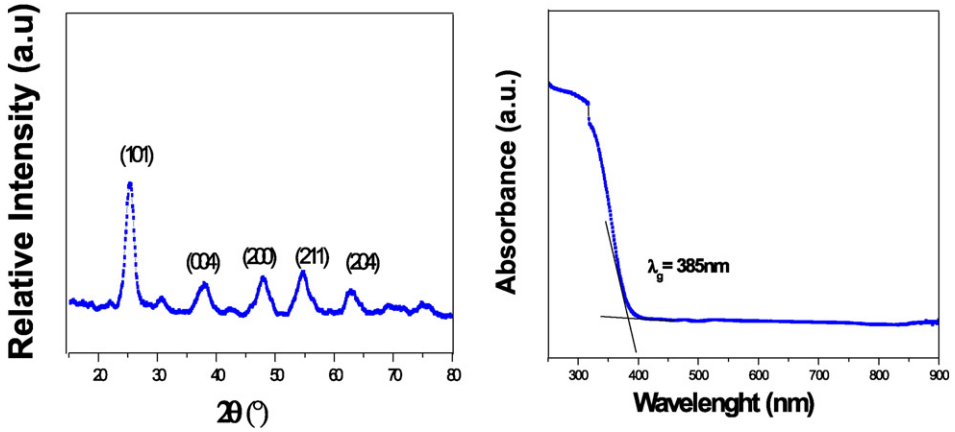

Fig. 2. XRD diffraction and UV spectra of (a) TiO_2 nanospheres.

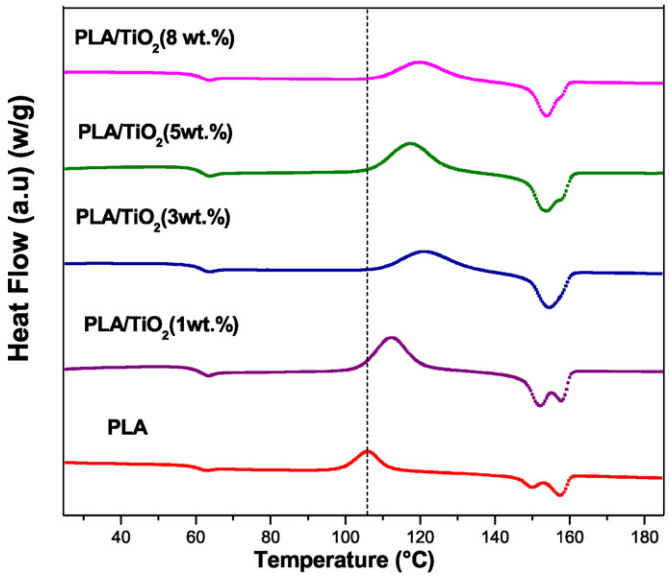

Fig. 3. DSC thermograms at the second heating scan of neat PLA and PLA/TiO_2 nanocomposites with different TiO_2 amounts.

endothermic process is related to the melting of meso-stable crystals formed during the cooling process. Immediately after this melting process, and overlapping with it, an exothermic process occurs (re-crystallization), forming more stable crystals that melt afterward, explaining the high-temperature endothermic peak. PLA crystals have therefore a great tendency to reorganize into more stable structures through this continuous melting–recrystallization–perfection (MRCM) mechanism during heating. Consequently, the small or imperfect crystals created during previous cooling could reorganize, resulting in a multiple melting behaviour [24]. With the increased amount of incorporated nanoparticles the polymers presented changes in the relative intensities of the double melting peaks. In general, the presence of the nanoparticles increases the low endothermic peak and at high concentration both merge. It is well known that MRCRM processes are retarded by high heating rates, as the time available for the diffusion of the molecular segments onto the growing re-crystallizing lamellae is shorter, reducing the high temperature melting peak [28]. Therefore, the presence of nanoparticles can restrict the motion of the polymer chains or segments, reducing or slowing down their ability to re-crystallize during heating [29]. The same conclusion was stated previously based on syndiotactic polymers [30]. On the other hand, with the incorporation of TiO_2 the melting temperature decreased slightly, and similar results were found for PLA/SiO_2 nanocomposites in comparison with neat PLA. The explanation was that the inclusion of nanosilica brought about smaller spherulites which may have more defects, resulting in a decrease of the melting temperature of the PLA/SiO_2 composite [31].

The effect of the spherulite growth process on PLA was examined in a polarized optical microscope, as shown in Fig. 4. The samples showed a Maltese cross pattern characteristic of the polymer crystallized in spherulites. The presence of nanoparticles increased the number of

Table 1
Thermal properties of PLA/TiO_2 nanocomposites.

Sample	TiO_2	Tg	Tc	T_{m1}	T_{m2}	X_c
	(wt.-%)	(°C)	(°C)	(°C)	(°C)	(%)
PLA	0	58	106	150	157	28
PLA/TiO_2	1	58	112	151	158	27
	3	59	121	–	154	31
	5	59	118	–	153	27
	8	59	120	–	154	28

Tg: glass transition temperature, Tc: crystallization temperature, T_m: melting temperature; X_c: percent crystallinity.

Table 2
Intrinsic viscosity and viscosity molecular weight and mechanical properties of PLA/TiO_2 nanocomposites.

Sample	TiO_2 content	η	Mv	E	ε_B
	(wt%)	(g/L)	(g/mol)	(MPa)	(%)
PLA	N/A	116	36,335	1079 ± 93	11.5 ± 0.40
PLA/TiO_2	1	–	–	1057 ± 58	8.4 ± 0.18
	3			1298 ± 92	5.5 ± 0.14
	5	54	12,802	1634 ± 43	5.8 ± 0,11
	8	74	19,615	1447 ± 59	7.4 ± 0.18

η: Viscosity, Mv: viscosity molecular weight, E = Young's modulus; ε_B = deformation at break.

spherulites, meaning both higher nucleation density and smaller size compared with neat PLA. This result confirmed the fact that TiO_2 nanoparticles increased the number of PLA spherulite cores, supporting the DSC results (Fig. 3). Nanoparticles in the polymer melt can reduce both the work required to create a new surface and the nucleus size for crystal growth. This behaviour occurs because the interface between the polymer crystal and the filler may be less hindered, so the creation of the corresponding free polymer crystal surface increases the nucleation density of the spherulites [32]. Therefore, a heterogeneous nucleation path reduces the free energy opposing the primary nucleation provided by the pre-existing surface of the filler. The increased spherulite density can be related to the spatial confinement of the precursor unit between adjacent nanoparticles, hindering the diffusive mobility of precursor unit clusters [33].

The effect of the addition of TiO_2 nanoparticles on the thermal stability of PLA-based nanocomposites was studied by TGA in a nitrogen atmosphere. The derivative DTG curves are displayed in Fig. 5. All materials showed a main peak associated with the PLA thermal degradation at 360 °C [34]. With the nanoparticle incorporations the nanocomposites did not present a significant change in the maximum degradation temperature.

The intrinsic viscosity and molecular weight of PLA and PLA/TiO_2 nanocomposites are displayed in Table 2. The viscosity molecular weight decreased with nanoparticle incorporation. Similar results were found by Giada Lo Re [35]. This behaviour may be due to very slight degradation of the PLA which can be attributed to a thermo-mechanical and hydrolysis reaction under the processing conditions. The average molecular weight reduction is smaller for 8 wt.% compared to 5 wt.% TiO_2 content formulation, as will be indicated later, probably due to the lubricant effect of the nanoparticles that improve the melt flow of nanocomposites, and that decreases the degradation effect of the PLA due to the nanocomposite preparation process [36].

2.1.2. Rheometry properties

The Fig. 6 shows the shear viscosity as a function of the shear rate of the neat PLA and PLA/TiO_2 nanocomposites melt with various contents of TiO_2 nanoparticles. The PLA matrix and its nanocomposites displayed pseudoplastic behaviour with a viscosity decreasing with the shear rate. The nanoparticles drastically decrease the viscosity of the polymer matrix, especially at low shear rate. This tendency is confirmed with data from viscosimeter tests for polymer solutions as displayed in Table 1. The viscosity drop can be associated with two effects: degradation of the PLA matrix during nanocomposite preparation, as explained above, or the lubricant effect of TiO_2 nanoparticles improving the mobility and flow of macromolecular chains in the melt. However, as the same tendency is found in polymer solutions, we can state that the degradation of the polymer is the mechanism for the decreased viscosity [37]. Some authors found the same behaviour for PLA/talc nanocomposites with 3.5 and 7 wt.% of the mineral filler compared to pure PLA [36]. Chan L. et al. reported also that the use of TiO_2 nanoparticles in epoxy composites reduced their frictional coefficient and improved their wear resistance properties [37]. The surface coating of the TiO_2 nanoparticles with stearic acid greatly reduced the shear viscosity values of

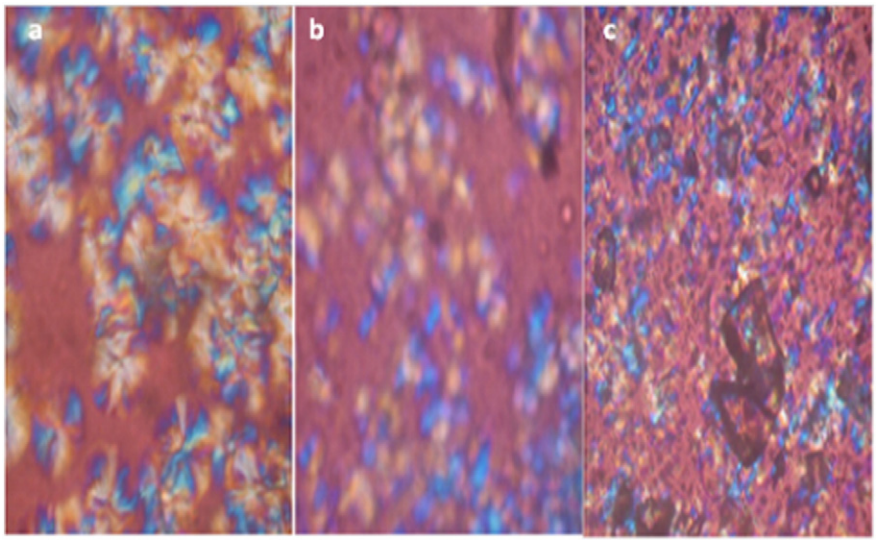

Fig. 4. Optical micrographs showing the nucleating effect of TiO_2 nanoparticles on PLA crystallization at 30 min. a) PLA, b) PLA/TiO_2 (1%wt.) and c) PLA/TiO_2 (8%wt.).

the composites compared to neat PLA [26]. The authors explain this behaviour caused by nanoparticles should be the result of the lubricating effect of stearic acid, which helps prevent the particles from aggregating and promotes the distribution of the particles within the melt.

A general tendency about the effect of nanoparticles on the rheological behaviour of the polymer was not found, as it depends on the characteristics of the particles and polymer. For instance, Supaphol et al. [38] found that for Polypropylene/TiO_2 nanocomposites the variation in nanoparticle content did not seem to have much effect on the shear viscosity values of the filled iPP melts. On the contrary, it was also reported that an increase of the shear viscosity values of the iPP melts with SiO_2-coated TiO_2 nanoparticles could be a result of the ability of the iPP molecules to be adsorbed on the particle surface [39]. PLA/clay nanocomposites also presented a shear viscosity increase with the incorporation of the nanoparticles, and it was attributed to the flow restrictions of PLA chains caused by the strong interaction between clay and PLA [40].

2.1.3. Mechanical properties

Regarding the mechanical properties displayed in the Table 2, the TiO_2 nanoparticles give rigidity to the polymer. The Young's PLA modulus increased upon addition of TiO_2 nanoparticles, whereas the strength increase indicates good interfacial adhesion between the matrix and the nanoparticles, and stress transfer of TiO_2 particles to the polymer [41]. The increase of Young's modulus may be related to the good dispersion of the TiO_2 nanoparticles in the PLA, as confirmed by TEM images [42,40].

A recent study has reported PLA surface energy (62.0 $mN{\cdot}m^{-1}$) and polar characters which are similar to those of TiO_2 (80.7 $mN{\cdot}m^{-1}$) [43]. The authors explained the good dispersion of TiO_2 in the PLA matrix as due to low interfacial tension between them. It has also been shown that C = O and C–O bonds, which are characteristic of the PLA structure, enhance the interaction with TiO_2 nanoparticles [44], and as a consequence good interfacial adhesion between the matrix and nanoparticles is expected. Young's modulus of PLA/TiO_2 nanocomposites increased up to 55% with 5 wt.% of TiO_2 nanoparticles compared with neat PLA. Similar mechanical properties improvement was found by Chen et al. [45] when 20 wt.% of organic layered double hydroxides (LDHs) were added to low density polyethylene. Wu J. et al. [31] reported that with the inclusion of nanofillers like SiO_2 in PLA can increase Young's modulus of the resulting polymer composite, basing their studies on the rule of mixtures (ROM).

On the other hand, elongation at break decreased with nanoparticle incorporations. In general, crystallization of semi-crystalline polymers results in embrittlement of the polymer, thereby decreasing the strain

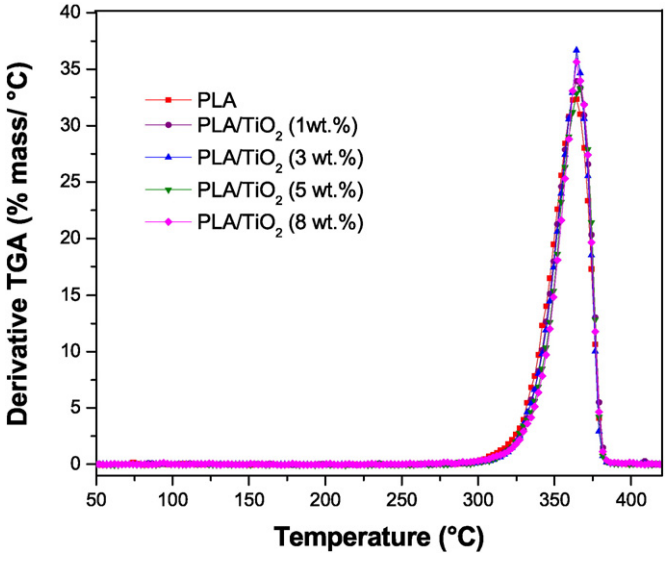

Fig. 5. Derivative TGA for the different PLA, PLA/TiO_2 nanocomposites with 1, 3, 5 and 8 wt.% of TiO_2 measured in inert atmosphere.

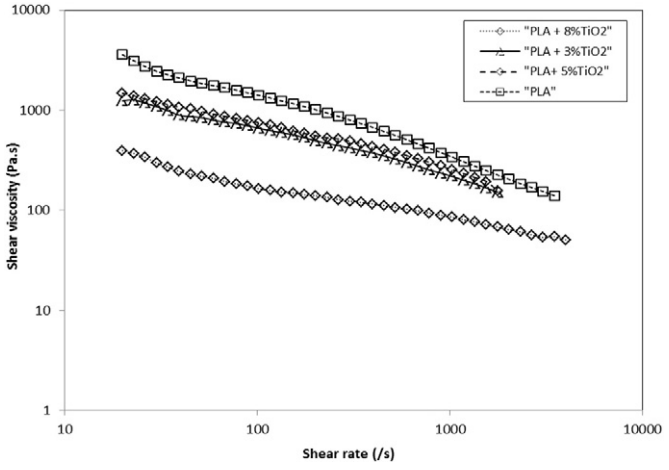

Fig. 6. Shear viscosity curves of PLA and PLA nanocomposites containing 3, 5, and 8 wt.% TiO_2 nanoparticles.

Table 3
Reduction percentage of the *E.coli* and *A. fungimatus* of PLA/TiO_2 nanocomposites.

Escherichia coli		% bacterial reduction	
Sample	TiO_2 (wt.%)	White light	UV light
PLA/TiO_2	5	10.0	29.4
	8	82.4	94.3
Aspergillus fumigatus ChFC 166-1		% fungal reduction	
Sample	TiO_2 (wt.%)	White light	UV light
PLA/TiO_2	5	9.2	66.7
	8	52.6	99.9

at break [46]. Similar results were found when PLA was reinforced with cellulose nanofibers (CNFs) [47].

2.1.4. Biocidal and antifungal properties

The results of the antimicrobial and antifungal properties against *E. coli* and *A. fumigatus* of the different PLA composites irradiated with white light and UVA are shown in Table 3. PLA/TiO_2 composites have shown a biocidal and antifungal behaviour that was increased with nanoparticle concentration and UV irradiation. The effectiveness against bacteria and fungi reached ~94.3% and 99.9% reduction, respectively, for PLA/TiO_2 nanocomposites containing 8 wt.% of TiO_2 and under UV irradiations. The inactivation of different bacteria and the cell-killing mechanisms by TiO_2 irradiated with UVA light have been reported [48]. By UV irradiation reactive species such as hydrogen peroxide, hydroxyl radical and superoxide anions cause cell death by decomposition of the cell wall first, followed by decomposition of the cell membrane [49]. Sunada et al. [50] explained that the process of *E. coli* photokilling is due to partial decomposition of the outer membrane by reactive species produced by TiO_2 photocatalysis. The partial decomposition of the membranes changes the permeability to reactive species, leading to the peroxidation of membrane lipids, the loss of cell viability, and cell death. This killing effect of the TiO_2 photocatalytic reaction has also been found on other cell types such as fungi, yeasts, viruses, or cancer cells. It is worth noting that PLA/TiO_2 nanocomposites containing 8 wt.% of TiO_2 nanoparticles are effective against bacteria and fungi with 82.4% and 52.6% reduction, respectively, regardless of UVA irradiation. Chawengskijwanich C. et al. [51] concluded that the extent of *E. coli* inactivation of TiO_2-film was relevant to the UVA intensity and kind of artificial light sources. Our experiments were carried out at low intensity (0.2 mW/cm^2), and PLA/TiO_2 nanocomposites show dependence of TiO_2 concentration; with 8 wt.% of TiO_2 the PLA/TiO_2 nanocomposites presented a good behaviour without UV irradiation. These results may be due to the small size of TiO_2 nanoparticles (diameter ca. 10 nm) and their good distribution in the PLA matrix. Its had been reported that the available TiO_2 surface area and dispersion homogeneity within the polymer matrix are key features in optimizing biokilling activity in our nanocomposite materials [6]. It is known that particle size affects the antimicrobial and antifungal behaviour regardless of the biocide mechanism. For instance, Damman et al. observed that the nanocomposites of PA6 (polyamide)/Ag exhibited a much higher antimicrobial efficacy than the microcomposites. In this case, the greater activity of the nanoparticles was explained by their more efficient silver ion release because of their much larger specific surface area [52]. Bahloul W. et al. [53] further mentioned the influence of TiO2 size, with smaller nanoparticles presenting the larger biocidal behaviour, as they can induce oxidative stress in the absence of photoactivation, and cell death without UV irradiation. Gur et al. [54] reported that in the absence of photoactivation TiO_2 may induce increased oxidative damage related to the concentration of hydrogen peroxide. These properties and all the results presented in this work suggest that these types of materials have a tremendous potential in food packaging and medicinal applications.

3. Conclusions

Poly(lactic acid) (PLA) composites with titanium oxide (TiO_2) nanoparticles were produced by the melting process. The crystallinity temperature increased ~12% when 5 wt.% of TiO_2 were added, and the TiO_2 nanoparticles increased the core number of PLA spherulites. Regarding mechanical properties, the elastic modulus of PLA/TiO_2 nanocomposites with 5 wt.% also increased ~54% compared to processed PLA, and this can be related to good distribution of the nanoparticles in the PLA matrix, verified by TEM analysis. It is notorious that the PLA/TiO_2 composite showed a reduction of *E. coli* and *A. fumigatus* of 94.3% and 99.9%, respectively. Therefore, these systems are attractive for use in food packaging or medical devices.

References

[1] I. Armentano, N. Bitinis, E. Fortunati, S. Mattioli, N. Rescignano, R. Verdejo, M.A. Lopez-Manchado, J.M. Kenny, Multifunctional nanostructured PLA materials for packaging and tissue engineering, Prog. Polym. Sci. 38 (2013) 1720–1747.
[2] Y. Luo, X. Wang, Y. Wang, Effect of TiO_2 nanoparticles on the long-term hydrolytic degradation behavior of PLA, Polym. Degrad. Stab. 97 (2012) 721–728.
[3] J.M. Raquez, Y. Habibi, M. Murariu, P. Dubois, Polylactide (PLA)-based nanocomposites, Prog. Polym. Sci. 38 (2013) 1504–1542.
[4] R.M. Rasal, A.V. Janorkar, D.E. Hirt, Poly(lactic acid) modifications, Prog. Polym. Sci. 35 (2010) 338–356.
[5] K. Fukushima, E. Giménez, L. Cabedo, J.M. Lagarón, J.L. Feijoo, Biotic degradation of poly(DL-lactide) based nanocomposites, Polym. Degrad. Stab. 97 (2012) 1278–1284.
[6] A. Kubacka, C. Serrano, M. Ferrer, H. Lu1nsdorf, P. Bielecki, M.L. Cerrada, M. Fernández-García, M. Fernández-García, High-performance dual-action polymer–TiO2 nanocomposite films via melting processing, Nano Lett. 7 (2007) 2529–2534.
[7] P.A. Zapata, L. Tamayo, M. Páez, E. Cerda, I. Azocar, F.M. Rabagliati, Nanocomposites based on polyethylene and nanosilver particles produced by metallocenic "in situ" polymerization: synthesis, characterization, and antimicrobial behavior, Eur. Polym. J. 47 (2011) 1541–1549.
[8] H. Palza, S. Gutierrez, O. Salazar, V. Fuenzalida, J. Avila, G. Figueroa, R. Quijada, Toward tailor-made biocide materials based on polypropylene/copper nanoparticles, Macromol. Rapid Commun. 31 (2010) 563–567.
[9] P.A. Zapata, H. Palza, F.M. Rabagliati, Novel antimicrobial polyethylene composites prepared by metallocenic "in-situ" polymerization with TiO_2 based nanoparticles, J. Polym. Sci. A Polym. Chem. 50 (2012) 4055–4062.
[10] H. Li, F. Li, L. Wang, J. Sehng, Z. Xin, L. Zhao, X H., Y. Zheng, Q. Hu, Effect of nano-packing on preservation quality of Chinese jujube (Ziziphus jujube Mill.var. inermis (Bunge) Rehd), Food Chem. 114 (2009) 547–552.
[11] A. Kubacka, M. Ferrer, M.L. Cerrada, C. Serrano, M. Sánchez-Chaves, M. Fernández-García, A. de Andrés, R. Jiménez, F. Fernández-Martín, Boosting TiO_2-anatase antimicrobial activity: polymer-oxide thin films, Appl. Catal. B Environ. 89 (2009) 441–447.
[12] D. Yañez, S. Guerrero, I. Lieberwirth, M.T. Ulloa, T. Gomez, F.M. Rabagliati, P.A. Zapata, Photocatalytic inhibition of bacteria by TiO_2 nanotubes-doped polyethylene, Appl. Catal. A Gen. 489 (2015) 255–261.
[13] A. Dural-Erem, Erem H. Hakan, G. Ozcan, M. Skrifvars, Anatase titanium dioxide loaded polylactide membranous films: preparation, characterization, and antibacterial activity assessment, Journal of the Textile Institute, 2014 http://dx.doi.org/10.1080/00405000.2014.929274.
[14] Y.B. Luo, W.D. Li, X.L. Wang, D.Y. Xu, Y.Z. Wang, Preparation and properties of nanocomposites based on poly(lactic acid) and functionalized TiO_2, Acta Mater. 57 (2009) 3182–3191.
[15] Y. Li, C. Chen, J. Li, X.S. Sun, Synthesis and characterization of bionanocomposites of poly(lactic acid) and TiO_2 nanowires by in situ polymerization, Polymer 52 (2011) 2367–2375.
[16] Y. Li, C. Chen, J. Li, X. Sun, Photoactivity of poly(lactic acid) nanocomposites modulated by TiO_2 nanofillers, J. Appl. Polym. Sci. (2014)http://dx.doi.org/10.1002/APP.40241.
[17] L.S. Cruz, H. Palza, F.M. Rabagliati, P.A. Zapata, Polyethylene and poly(ethylene-co-1-octadecene) composites with TiO_2 based nanoparticles by metallocenic "in situ" polymerization, Polymer 54 (2013) 2690–2698.
[18] M.I. Mejia, J.M. Marín, G. Restrepo, L.A. Rios, C.J. Pulgarín, Preparation, testing and performance of a TiO2/polyester photocatalyst for the degradation of gaseous methanol, Appl. Catal. B Environ. 94 (2010) 166–172.
[19] CLSI: Clinical and Laboratory Standards Institute, Reference method for broth dilution antifungal susceptibility testing of filamentous fungi, Approved standard-second edition. CLSI document M38-A2. , Clinical and Laboratory Standards Institute, Wayne, PA, 2008.
[20] P.K. Khanna, N. Singh, S. Charan, Synthesis of nano-particle s of anatase-TiO2 and preparation of its optically transparent film in PVA, Mater. Lett. 61 (2007) 4725–4730.
[21] K. László, D. Imre, Colloids Surf. A Physicochem. Eng. Asp. 280 (2006) 146–154.
[22] M.I. Mejia, J.M. Marín, G. Restrepo, L.A. Rios, C. Pulgarín, Preparation, testing and performance of a TiO_2/polyester photocatalyst for the degradation of gaseous methano, Appl. Catal. B Environ. 94 (2010) 166–172.

[23] X. Gong, L. Pan, C. Tang, L. Chen, Z. Hao, W. Law, X. Wang, C. Tsui, C. Wu, Preparation, optical and thermal properties of CdSe–ZnS/poly(lactic acid) (PLA) nanocomposites, Compos. Part B 66 (2014) 494–499.
[24] A. Frone, S. Berlioz, J. Chailan, D. Panaitescu, Morphology and thermal properties of PLA-cellulose nanofibers composites, Carbohydr. Polym. 91 (2013) 377–384.
[25] A. Araújo, G. Botelho, M. Oliveira, A.V. Machado, Influence of clay organic modifier on the thermal-stability of PLA based nanocomposites, Appl. Clay Sci. 88–89 (2014) 144–150.
[26] G.X. Zou, Q.W. Jiao, X. Zhang, C.X. Zhao, J.C. Li, Crystallization behavior and morphology of poly (lactic acid) with a novel nucleating agent, J. Appl. Polym. Sci. (2015)http://dx.doi.org/10.1002/APP.41367.
[27] P. Pan, W. Kai, B. Zhu, T. Dong, Y. Inoue, Polymorphous crystallization and multiple melting behavior of poly (L-lactide): molecular weight dependence, Macromolecules 40 (2007) 6898–6905.
[28] P. Supaphol, Crystallization and melting behavior in syndiotactic polypropylene: origin of multiple melting phenomenon, J. Appl. Polym. Sci. 82 (2001) 1083–1097.
[29] M.L. Cerrada, V. Rodríguez-Amor, E. Perez, Effects of clay nanoparticles and electron irradiation in the crystallization rate of syndiotactic polypropylene, J. Polym. Sci. B Polym. Phys. 45 (2007) 1068–1076.
[30] A. Zurita, H. Palza, Effect of the polymer microstructure on the behavior of syndiotactic polypropylene/organophilic layered silicate composites, J. Appl. Polym. Sci. 124 (2012) 2601–2609.
[31] J. Wu, S.Y. Yen, M.C. Kuo, B. Chen, Physical properties and crystallization behavior of silica particulates reinforced poly(lactic acid) composites, Mater. Chem. Phys. 142 (2013) 726–733.
[32] M. Mucha, Z. Królikowski, Application of dsc to study crystallization kinetics of polypropylene containing filler, J. Therm. Anal. Calorim. 74 (2003) 549–557.
[33] K. Nitta, K. Asuka, B. Liu, M. Terano, The effect of the addition of silica particles on linear spherulite growth rate of isotactic polypropylene and its explanation by lamellar, Polymer 47 (2006) 6457–6463.
[34] M. Ramos, E. Fortunati, M. Peltzer, F. Dominici, A. Jiménez, M.C. Garrigós, J.M. Kenny, Influence of thymol and silver nanoparticles on the degradation of poly(lactic acid) based nanocomposites: thermal and morphological properties, Polym. Degrad. Stab. 108 (2014) 158–165.
[35] G. Re, S. Benali, Y. Habibi, J.M. Raquez, P. Dubois, Stereocomplexed PLA nanocomposites: from in situ polymerization to materials properties, Eur. Polym. J. 54 (2014) 138–150.
[36] C. Cipriano, A. Nazareth da Silva, A. Monteiro da Fonseca, T. da Silva, A. Furtado de Sousa, G. Monteiro da Silva, C. Rabello do Nascimento, Rheological and morphological properties of composites based on polylactide and talc, J. Mater. Sci. Eng. B 3 (11) (2013) 695–699.
[37] L. Chang, Z. Zhan, C. Breidt, K. Friedrich, Tribological properties of epoxy nanocomposites I. Enhancement of the wear resistance by nano-TiO_2 particles, Wear 258 (2005) 141–148.
[38] R. Dangtungee, P. Supaphol, Melt rheology and extrudate swell of titanium (IV) oxide nanoparticle-filled isotactic polypropylene: effects of content and surface characteristics, Polym. Test. 27 (2008) 951–956.
[39] P. Supaphol, P. Thanomkiat, J. Junkasem, R. Dangtungee, Polymer testing, Non-isothermal melt-crystallization and mechanical properties of titanium (IV) oxide nanoparticle-filled isotactic, Polypropylene 26 (2007) 20–37.
[40] Y. Di, S. Iannace, E. Di Maio, L. Nicolais, Poly(lactic acid)/organoclay nanocomposites: thermal, rheological properties and foam processing, J. Polym. Sci. B Polym. Phys. 43 (2005) 689–698.
[41] S. Lai, S. Wu, G. Lin, T. Don, Unusual mechanical properties of melt-blended poly(lactic acid) (PLA)/clay nanocomposites, Eur. Polym. J. 52 (2014) 193–206.
[42] F. Ciardelli, S. Coiali, E. Passaglia, A. Pucci, G. Ruggeri, Nanocomposites based on polyolefins and functional thermoplastic materials, Polym. Int. 57 (2008) 805–836.
[43] J.P. Mofokeng, A.S. Luyt, Morphology and thermal degradation studies of melt-mixed PLA/PHBV biodegradable polymer blend nanocomposites with TiO_2 as filler, J. Appl. Polym. Sci. (2015)http://dx.doi.org/10.1002/APP.42138.
[44] W. Chen, Ch. Qian, X.-Y. Liu, H.-Q. Yu, Two-dimensional correlation spectroscopic analysis on the interaction between humic acids and TiO_2 nanoparticles, Environ. Sci. Technol. 48 (2014) 11119–11126.
[45] W. Chen, B. Qu, LLDPE/ZnAl LDH-exfoliated nanocomposites: effects of nanolayers on thermal and mechanical properties, J. Mater. Chem. 14 (2004) 1705–1710.
[46] L. Suryanegara, A. Nakagaito, H. Yano, The effect of crystallization of PLA on the thermal and mechanical properties of microfibrillated cellulose-reinforced PLA composites, Compos. Sci. Technol. 69 (2009) 1187–1192.
[47] M. Jonoobi, J. Harun, A. Mathew, K. Oksman, Mechanical properties of cellulose nanofiber (CNF) reinforced polylactic acid (PLA) prepared by twin screw extrusion, Compos. Sci. Technol. 70 (2010) 1742–1747.
[48] G. Fu, P.S. Vary, Ch-T. Lin, Anatase TiO2 nanocomposites for antimicrobial coatings, J. Phys. Chem. B 109 (2005) 8889–8898.
[49] Z. Lu, L. Zhou, Z. Zhang, W. Shi, Z. Xie, H. Xie, D. Pang, P. Shen, Cell damage induced by photocatalysis of TiO_2 thin films, Langmuir 19 (2003) 8765–8768.
[50] K. Sunada, T. Watanabe, K. Hashimoto, Studies on photokilling of bacteria on TiO_2 thin film, J. Photochem. Photobiol. A Chem. 156 (2003) 227–233.
[51] C. Chawengskijwanich, Y. Hayata, Development of TiO_2 powder-coated food packaging film and its ability to inactive Escherichia coli in citro and in actual tests, Int. Food Micorbiol. 123 (2008) 288–292.
[52] C. Damm, H. Munstedt, A. Rosch, The antimicrobial efficacy of polyamide 6/silver-nano- and microcomposites, Mater. Chem. Phys. 108 (2008) 61–66.
[53] W. Bahloul, F. Mélis, V. Bounor-Legaré, P. Cassagnau, Structural characterization and antibacterial activity of PP/TiO2 nanocomposites prepared by in situ sol–gel method, Mater. Chem. Phys. 134 (2012) 399–406.
[54] J.R. Gurr, A.S.S. Wang, C.H. Chan, K.Y. Jan, Ultrafine titanium dioxide particle in the absence of photoactivation can induce oxidative damage to human bronchial epithelial cells, Toxycology 213 (2005) 66–73.